arXiv:1602.06721v1 [cond-mat.mtrl-sci] 22 Feb 2016

Local Structure and Spin Transition in Fe_2O_3 Hematite at High-Pressure

Andrea Sanson,[1,*] Innokenty Kantor,[2] Valerio Cerantola,[2] Tetsuo Irifune,[3] Alberto Carnera,[1] and Sakura Pascarelli[2]

[1] *Department of Physics and Astronomy - University of Padova, Padua (Italy)*
[2] *ESRF - European Synchrotron Radiation Facility, Grenoble (France)*
[3] *Geodynamic Research Center - University of Ehime, Matsuyama (Japan)*

(Dated: February 23, 2016)

The pressure evolution of the local structure of Fe_2O_3 hematite has been determined for the first time by extended x-ray absorption fine structure up to ∼79 GPa. The comparison to the different high-pressure forms proposed in the literature suggests that the orthorhombic structure with space group *Aba2* is the most probable. The crossover from Fe high-spin to low-spin states with pressure increase has been monitored from the pre-edge region of the Fe K-edge absorption spectra. The "simultaneous" comparison with the local structural changes allows us to definitively conclude that it is the electronic transition that drives the structural transition and not viceversa.

The high-pressure behavior of hematite (α-Fe_2O_3) has raised much debate in the scientific community over the past decades. At ambient conditions, hematite crystallizes in the rhombohedral corundum-type structure, space group $R\overline{3}c$, and is a wide-band antiferromagnetic insulator. By increasing pressure at room temperature, the corundum structure of hematite is progressively distorted and, above ∼50 GPa, a series of physical changes occur [1–11]: the unit cell volume drops down by about 10 %, the crystal symmetry changes completely, the electrical resistivity decreases drastically due to the breakdown of the *d*-electron correlation (Mott insulator-metal transition), the magnetic moments collapse [transition of iron ions from high-spin (HS) to low-spin (LS) state] and the long-range magnetic order disappears. Besides being interesting from the viewpoint of solid-state physics, the phenomena are also important in geophysics for modeling materials behavior in deep Earth's mantle [12–16].

Despite many experimental and theoretical studies have been conducted on this issue, several aspects still remain controversial and unsolved. From the structural point of view, it was initially proposed that the high-pressure (HP) form of Fe_2O_3 was a $GdFeO_3$-type orthorhombic perovskite, containing two different Fe sites with different coordination numbers and characterized by unequal valence states, i.e., Fe^{2+} and Fe^{4+} [17–19]. But a few years later, further investigations established that the HP phase of Fe_2O_3 is a non-magnetic metallic phase with a single Fe^{3+} cation site, and identified as the distorted Rh_2O_3-II structure [4–6]. However this conclusion cannot be regarded as definitive because not based on x-ray "single-crystal" diffraction data, that provides the most accurate structural refinement, and moreover because certain aspects have been challenged by Badro and co-workers [2]. In confirmation of this, a recent synchrotron x-ray single-crystal diffraction study proposes that, in the mixed state above 50 GPa, Fe_2O_3 forms a novel monoclinic phase with space group $P2_1/n$ and, above 67 GPa, compression triggers the transition to a different HP phase with orthorhombic unit cell and space group *Aba2* [20, 21]. Another important and controversial point refers to the nature of the phase-transition at ∼50 GPa: is it the structural transition that drives the electronic transition or viceversa? Some authors stated that the structural transition precedes the change in the electronic properties of Fe_2O_3 [2, 3], while other authors proposed the opposite scenario [5–9]. Different theoretical approaches lead to different and controversial results.

All these unsolved issues stimulate new high pressure studies of hematite by means of other techniques. One of these is extended x-ray absorption fine structure (EXAFS) spectroscopy that, thanks to its selectivity to atomic species and insensitivity to long range order, is a powerful tool for the study of local structure and electronic properties of solids [22]. However, many difficulties are associated with conducting EXAFS studies at high-pressure, due to the strong absorption of the diamond anvils at low x-ray energies (the Fe K-edge is at 7.1 KeV), and due to intrinsic limitations to the measurable k-range for EXAFS because of Bragg diffraction from the diamonds. In this study, Fe K-edge energy dispersive EXAFS measurements have been conducted on Fe_2O_3 under pressures up to ∼79 GPa (and then decompressing up to ∼19 GPa) at the ID24 XAS beamline of the European Synchrotron Radiation Facility (ESRF) in Grenoble [23]. The recent developments on this beamline, together with the availability of nanodiamond anvils [24], offer the possibility to reach a larger k-range (up to about 10 $Å^{-1}$ in the present study) at very high pressures [25, 26].

The experimental details and data analysis are provided in the Supplemental Material [28]. Due to the large number of distances involved, the nearest-neighbor Fe-O distances were assumed to follow one single-peak average distribution. The validity of this assumption was tested in Ref. [27] and is also confirmed by the subsequent agreement with the crystallographic data of hematite. The same assumption was made for the analysis of the next-nearest-neighbor Fe-Fe/O distances. However, in the latter case, the situation is much more complicated because the number (and type) of atoms in the outer-shells is not well defined as in the first-shell, where the

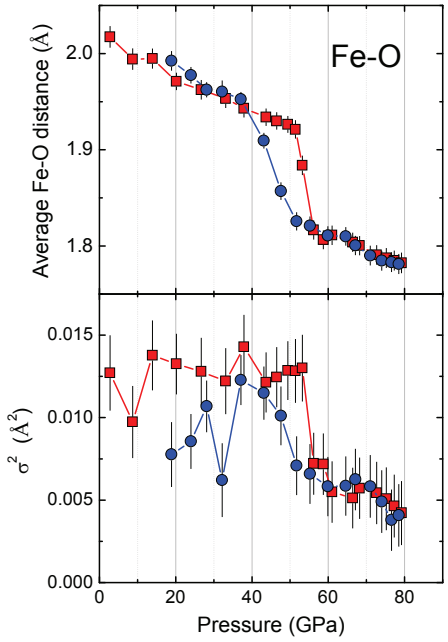

FIG. 1: Pressure-dependence of the average Fe-O distance (top panel) and of the variance σ^2 of corresponding Fe-O distribution (bottom panel). Red squares and blue circles refer to compression and decompression, respectively. The solid lines are guide to the eyes.

Fe atoms are coordinated by 6 oxygens (within a bonding distance of 2.3 Å) in all the proposed HP structures of Fe_2O_3 as in the simple corundum structure. Accordingly, we will focus our attention on the nearest-neighbor Fe-O distances. The results for the next-nearest-neighbor Fe-Fe/O distances are reported and discussed in the Supplemental Material [28].

The resulting average Fe-O distance as a function of pressure is shown in the top panel of Fig. 1. The bottom panel of the same figure shows instead the pressure dependence of variance σ^2 of the corresponding average distance distribution. As expected, it can be seen that the Fe-O distance progressively decreases with increasing pressure (red squares), and, above ∼50 GPa, we observe an abrupt decrease (of about 0.1 Å) which reveals the HP phase transition of Fe_2O_3. Very interesting is the behavior of σ^2 above the transition, indicating a sharp decrease of the static disorder in the nearest-neighbor Fe-O distances, consistent with a reduction in the distortion of the FeO_6 octahedra. Finally, during decompression, a hysteresis effect is observed across the phase transition (blue circles in Fig. 1), although we do not have direct evidence that the phase obtained upon decompression is identical to the initial one. Indeed the σ^2 deviates somewhat from that measured upon compression, and this could be linked to different distortion of the FeO_6 octahedra.

Fig. 2 shows the average Fe-O distance distributions at

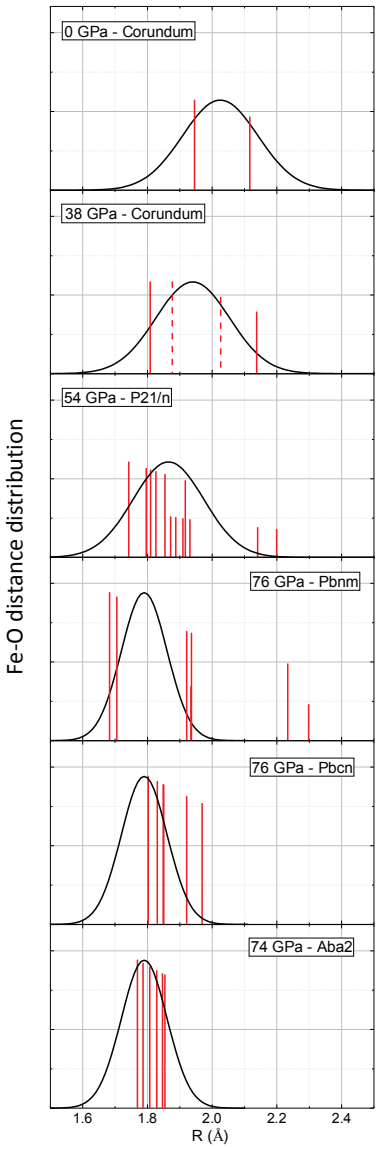

FIG. 2: Fe-O average distributions determined by EXAFS (black-solid lines). The red bars indicate the Fe-O distances according to the HP structures proposed in literature. The red-dashed vertical bars in the second panel from the top are the Fe-O distances of hematite by assuming unchanged the atomic positions in the unit cell.

the pressures of interest for our next discussion, roughly approximated to Gaussian distributions in accordance to the data of Fig. 1. The vertical bars indicate the Fe-O distances according to the HP structures proposed in literature [4–6, 17–21]. Their heights were scaled according to the EXAFS amplitude calculated by the FEFF code [29, 30] at 0 K (atoms frozen in their equilibrium positions) and arbitrarily normalized to the height of the Fe-O distributions.

The local structure results of Fig. 2, summarized in Tab. I, can help to shed light on the controversial HP phase of Fe_2O_3. Note that the EXAFS σ^2 reported in

TABLE I: Average Fe-O parameters expected for the different HP structures of Fe_2O_3 (left side) and their comparison with the experimental EXAFS results (right side). In order to do a more accurate comparison, the structural parameters were calculated by weighting the respective distances according to their EXAFS scattering-amplitudes, while the dynamic contribution to σ^2 was approximated to those of hematite at ambient conditions (see text).

Crystal Structure	Expected		EXAFS	
	Fe–O [Å]	σ^2_{Fe-O} [Å^2]	Fe–O [Å]	σ^2_{Fe-O} [Å^2]
Corundum (0 GPa)	2.02	0.013	2.02±0.01	0.013±0.002
Corundum A (38GPa)[a]	1.94	0.032	1.94±0.01	0.013±0.002
Corundum B (38GPa)	1.94	0.012	1.94±0.01	0.013±0.002
P21/n (54 GPa)[b]	1.87	0.017	1.87±0.01	0.012±0.002
Pbnm (76 GPa)[a,*]	1.81/1.88	0.020/0.046	1.79±0.01	0.005±0.002
Pbcn (76 GPa)[a]	1.87	0.009	1.79±0.01	0.005±0.002
Aba2 (74 GPa)[b]	1.81	0.007	1.79±0.01	0.005±0.002

a) crystal cell from Ref. [6], b) from Refs. [20, 21].
*the two set of values were obtained by neglecting or including the Fe-O distances at ∼2.3 Å, respectively.

the last column of Tab. I, is the sum of a static contribution σ^2_{st} due to the presence of Fe-O distances of different lengths, and a dynamic contribution σ^2_{din} due to thermal disorder. For the Fe-O nearest-neighbors of hematite at ambient conditions, σ^2_{st} is about 0.007 Å^2, while the average value of σ^2_{din}, determined by temperature-dependent EXAFS measurements and molecular dynamics calculations [31], is about 0.006 Å^2. In the determination of the expected σ^2 of the different HP structures, listed in the third column of Tab. I, we approximated the dynamic contribution σ^2_{din} to that of hematite at ambient conditions.

As first, we consider the HP structure before the transition proposed by Rozenberg and co-workers [6]. According to their refined structural parameters, the resulting average Fe-O distance is in very good agreement with that obtained in the present EXAFS study (2nd panel from the top of Fig. 2). However, Rozenberg *et al.* found that pressure induces a progressive distortion of the FeO_6 octahedron, in which the distance gap between short and long Fe-O nearest-neighbors progressively increases up to about 0.4 Å, resulting in a progressive increase of the static disorder σ^2_{st} up to ∼0.04 Å^2. This is in sharp contrast with our EXAFS results shown in the bottom panel of Fig. 1, where below the phase-transition σ^2 is constant and ∼0.013 Å^2. Accordingly, no further distortion of the FeO_6 octahedra is observed with increasing pressure with respect to the ambient conditions. To show this, the average Fe-O structural parameters were calculated from Rozenberg's refinement, for example at 38 GPa (Tab. I - Corundum A), and the same was done using the lattice parameters of Rozenberg *et al.* but leaving unchanged the atomic positions in the unit cell (Tab. I - Corundum B). It can be seen that the agreement with the experimental EXAFS data, specifically σ^2, is much better for the latter.

We now consider the HP structures of Fe_2O_3 above the phase transition. For the novel monoclinic phase (space group *P21/n*) proposed by Bykova *et al.* [20, 21] at 54 GPa, only the expected average Fe-O distance is in agreement with that of EXAFS (Tab. I, 4th row); in contrast, the value of σ^2 indicates a small, but not negligible, Fe-O distortion and therefore we cannot validate this HP structure. More enlightening is the comparison of the HP structures above 70 GPa. The local structural parameters of the $GdFeO_3$-type perovskite structure, space group *Pbnm*, are completely at odds with the EXAFS results (Tab. I, 5th row), independently on whether the Fe-O distances at 2.3 Å are included or not. In particular, the static disorder of the nearest-neighbor Fe-O distribution is too large compared to that measured by EXAFS, therefore, in agreement with previous studies [4–6, 15], we can rule out the $GdFeO_3$ form as HP structure of Fe_2O_3. However, we come to the same conclusion also for the distorted Rh_2O_3-II structure, space group *Pbcn*, which is currently the most accepted HP structure for Fe_2O_3 [4–6]. Indeed, from Tab. I - 6th row, the structural parameters of this form show a significant discrepancy with the EXAFS results. On the contrary, the best agreement seems to be found for the orthorhombic structure with space group *Aba2* (Tab. I, 7th row), the HP structure very recently proposed by Bykova and co-workers [20] on the basis of synchrotron x-ray single-crystal diffraction.

We now address the controversial issue of the nature of the phase-transition [2, 3, 5–9], i.e., do the electronic properties of Fe_2O_3 change only after the structural transition with a decrease in volume and a change in the lattice symmetry, or viceversa? In this regard, the evolution of the Fe 3d electronic structure vs pressure can be investigated from the pre-edge region of the Fe K-edge absorption spectrum (top panel of Fig. 3), since this pre-edge feature can be assigned to transitions to the t2g and eg components of the 3d band [11, 32] and, therefore, is

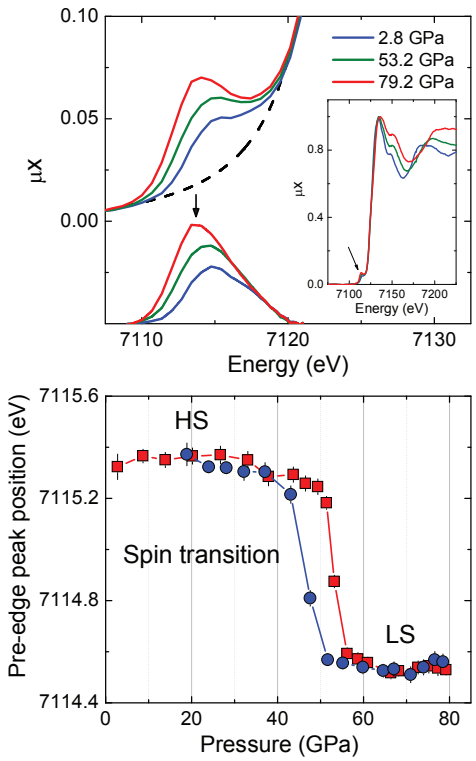

FIG. 3: Top panel: pre-edge peak of the Fe K-edge absorption spectra at selected pressures and corresponding background subtraction. The inset shows the whole absorption spectra. Bottom panel: Fe^{3+} high-spin/low-spin crossover monitored by the average pre-edge peak position as a function of pressure, during compression (red squares) and decompression (blue circles).

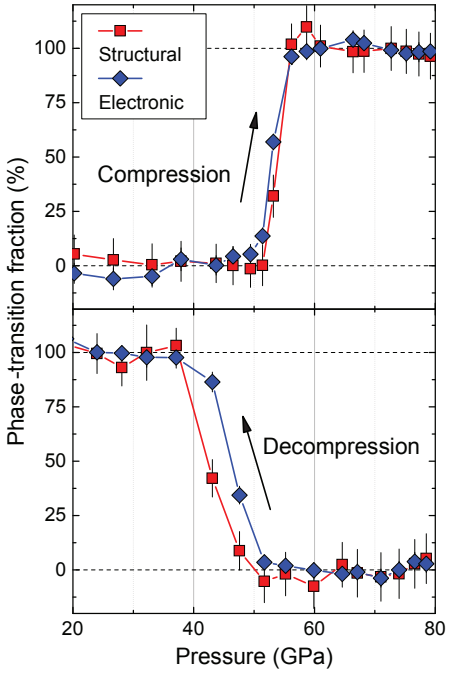

FIG. 4: Phase-transition fraction (in percent) during compression (top panel) and decompression (bottom panel). Red-squares refer to the structural transition, blue-diamonds to the electronic transition. In the both cases, the electronic transition precedes the structural transition.

directly connected to the population of the HS and LS states. After normalization and background subtraction of absorption spectra (top panel of Fig. 3), the average position of the pre-edge peak was determined and plotted as a function of pressure (bottom panel of Fig. 3): in this way we monitor the crossover from HS to LS states with pressure increase and viceversa.

The "simultaneous" measurement of the structural transition (Fig. 1) and of the electronic transition (Fig. 3) is fundamental to overcome the uncertainty due to different hydrostatic conditions and different measured volume, and allows addressing questions related to the interplay between structural and electronic/magnetic degrees of freedom in Fe_2O_3, as previously demonstrated for pure Fe [33]. In Fig. 4 we show the evolution of the phase-transition fraction, both structural and electronic, during compression (top panel) and decompression (bottom panel). During compression, in the mixed HS/LS state at about 53 GPa, the electronic transition is ∼60 % completed (blue diamonds in the top panel of Fig. 4), while the structural transition (red squares) is only ∼30 % completed. As a result, we can deduce that the HP structural transition occurs only after the electronic transition to the low-spin phase. Further confirmation of this finding is given by the data collected during decompression. At about 48 and 43 GPa, the LS to HS transition is completed at ∼35 % and ∼85 %, respectively (blue diamonds in the bottom panel of Fig. 4), while the structural transition (red squares) is only completed at ∼10 % and ∼40 %, respectively. This shows again that the electronic transition actually precedes the structural transition, and leads to the following description of the HP transition of Fe_2O_3: *i*) volume and bond distances decrease with pressure until a "volume threshold" value is reached at ∼50 GPa, in which the low-spin phase is more stable as predicted by some theoretical calculations [8, 9, 34]. The spin crossover transition from HS to LS states is thus activated *ii*) the full HS to LS transition occurs between ∼50 and 55 GPa. In this pressure interval, the sample enters into a metastable phase characterized by Fe^{3+} ions in the mixed HS/LS state, in which the crystal structure is still (at least initially) unchanged. Further increase in pressure triggers the Fe^{3+} ions into the stable LS phase, thus causing the structural transition and volume collapse (LS Fe atomic radius becomes ∼0.1 Å shorter than that of HS Fe [35]) as a consequence of emptying of the anti-bonding bands in the LS phase and corresponding strengthening of the Fe-O bonds [8] *iii*) above ∼55 GPa the Fe^{3+} are all (or almost) LS, and bond distances and volume continue to decrease as a mere

effect of pressure increase.

Summarizing, in this Letter we have studied the local structure of Fe_2O_3 hematite under high pressure. Below the phase transition, no increasing FeO_6 octahedra distortion is observed as pressure is applied, in contrast to Rozenberg et al. [6]. More importantly, an abrupt decrease in the nearest-neighbor Fe-O distance is observed at ∼50 GPa. Concomitantly, we observe a peculiar decrease of the nearest-neighbor Fe-O static disorder, indicating a reduction in the FeO_6 distortion. The present EXAFS results represent an excellent test-bench for proposed or new HP forms of Fe_2O_3. Comparison to the different HP phases proposed in the literature rules out the $GdFeO_3$-type orthorhombic perovskite form as well as the most accepted distorted Rh_2O_3-II structure, and rather suggests that the orthorhombic structure with space group *Aba2* is the most appropriate among those reported in literature.

Finally, the pressure-induced Fe^{3+} high-spin to low-spin transition has been monitored from the pre-edge peak of the Fe K-edge absorption spectra. The simultaneous comparison with the pressure evolution of the local structural transition determined by EXAFS allows us to conclude that it is the electronic transition that drives the structural transition and not viceversa, thus definitively solving the longstanding controversy on the nature of the phase-transition. The details of the dynamics of this phase transition, and in particular, the nature of the observed metastable phase, call for further theoretical and experimental investigations.

We acknowledge the European Synchrotron Radiation Facility (ESRF) for provision of synchrotron radiation, as well as E. Bykova, L. Dubrovinsky and O. Mathon for useful discussions. This work has been partially supported by the ESRF project No. HE-3766.

* Electronic address: andrea.sanson@unipd.it

[1] E. Knittle and R. Jeanloz, Solid State Commun. **58**, 129 (1986).
[2] J. Badro, G. Fiquet, V.V. Struzhkin, M. Somayazulu, H.K. Mao, G. Shen, T.L. Bihan, Phys. Rev. Lett. **89**, 205504 (2002).
[3] J.-F. Lin, J. S. Tse, E. E. Alp, J. Zhao, M. Lerche, W. Sturhahn, Y. Xiao, and P. Chow, Phys. Rev. B **84**, 064424 (2011).
[4] H. Liu, W. A. Caldwell, L. R. Benedetti, W. Panero, and R. Jeanloz, Phys. Chem. Minerals **30**, 582 (2003).
[5] M. P. Pasternak, G. Kh. Rozenberg, G. Yu. Machavariani, O. Naaman, R. D. Taylor, and R. Jeanloz, Phys. Rev. Lett. **82**, 4663 (1999).
[6] G. Kh. Rozenberg, L. S. Dubrovinsky, M. P. Pasternak, O. Naaman, T. Le Bihan, and R. Ahuja, Phys. Rev. B **65**, 064112 (2002).
[7] V. Kozhevnikov, A. V. Lukoyanov, V. I. Anisimov, and M. A. Korotin, J. Exp. and Theor. Phys. **105**, 1035 (2007).
[8] J. Kuneš, Dm. M. Korotin, M. A. Korotin, V. I. Anisimov, and P. Werner, Phys. Rev. Lett. **102**, 146402 (2009).
[9] D. B. Ghosh and S. de Gironcoli, arXiv:0905.3414.
[10] N.C. Wilson and S. P. Russo, Phys. Rev. B **79**, 094113 (2009).
[11] S. Wang *et al.*, Phys. Rev. B **82**, 144428 (2010).
[12] R.C. Liebermann and E. Schreiber, J. Geophys. Res. **73**, 6585 (1968).
[13] K.-I. Kondo, T. Mashimo, and A. Sawaoka, J. Geophys. Res. **85**, 977 (1980).
[14] T. Yagi and S. Akimoto, in *High-pressure research in Geophysics* (Kluwer Academic, Tokyo, 1982).
[15] S.-H. Shim and T. S. Duffy, Amer. Mineral. **87**, 318 (2002).
[16] S.-H. Shim, A. Bengtson, D. Morgan, W. Sturhahn, K. Catalli, J. Zhao, M. Lerche, and V. Prakapenka, Proc. Nat. Acad. Sci. **106**, 5508 (2009).
[17] T. Suzuki, T. Yagi, S. Akimoto, A. Ito, S. Morimoto, and T. Syono, in Solid State Physics under Pressure, edited by S. Minomura (KTK Scientific Publishers, Tokyo, 1985), p. 149.
[18] J. Staun Olsen, C. S. G. Cousins, L. Gerward, H. Jhans, and B. J. Sheldon, Phys. Scripta **43**, 327 (1991).
[19] Y. Syono, A. Ito, S. Morimoto, S. Suzuki, T. Yagi, and S. Akimoto, Solid State Commun. **50**, 97 (1984).
[20] E. Bykova *et al.*, Nature Comm. (2016), in press.
[21] E. Bykova, Maxim Bykov, V. Prakapenka, Z. Konpková, H.-P. Liermann, N. Dubrovinskaia, and L. Dubrovinsky, High Pressure Res. **33**, 534 (2013).
[22] A. E. Stern, *X-Ray Absorption: Principles, Applications, Techniques of EXAFS, SEXAFS and XANES* (New York: Wiley and Sons, 1988)
[23] S. Pascarelli *et al.*, J. Synchrotron Rad. **23**, 353 (2016).
[24] T. Irifune, A. Kurio, S. Sakamoto, T. Inoue and H. Sumiya, Nature **421**, 599 (2003).
[25] M. Baldini, W. Yang, G. Aquilanti, L. Zhang, Y. Ding, S. Pascarelli, and W. L. Mao, Phys. Rev. B **84**, 014111 (2011).
[26] R. Torchio, O. Mathon, and S. Pascarelli, Coord. Chem. Rev. **277278**, 80 (2014).
[27] A. Sanson, A. Zaltron, N. Argiolas, C. Sada, M. Bazzan, W. G. Schmidt and S. Sanna, Phys. Rev. B **91**, 094109 (2015).
[28] See Supplemental Material for details on experiment and data analysis.
[29] A. L. Ankudinov, B. Ravel, J. J. Rehr, and S. D. Conradson, Phys. Rev. B **58**, 7565 (1998).
[30] J.J. Rehr, J.J. Kas, F.D. Vila, M.P. Prange, K. Jorissen, Phys. Chem. Chem. Phys. **12**, 5503 (2010).
[31] A. Sanson, O. Mathon, and S. Pascarelli, J. Chem. Phys. **140**, 224504 (2014).
[32] W. A. Caliebe, C.-C. Kao, J. B. Hastings, M. Taguchi, A. Kotani, T. Uozumi, and F. M. F. de Groot, Phys. Rev. B **58**, 13452 (1998).
[33] O. Mathon, F. Baudelet, J. P. Itié, A. Polian, M. d'Astuto, J. C. Chervin, and S. Pascarelli, Phys. Rev. Lett. **93**, 255503 (2004).
[34] G. Rollmann, A. Rohrbach, P. Entel, and J. Hafner, Phys. Rev. B **69**, 165107 (2004).
[35] R. D. Shannon, Acta Cryst. **A32**, 751 (1976).